INSTITUTE OF PHYSICS PUBLISHING SEMICONDUCTOR SCIENCE AND TECHNOLOGY

Semicond. Sci. Technol. **19** (2004) S40–S42 PII: S0268-1242(04)71783-6

Relaxation oscillations in a bistable quantum Hall system

A Buß[1], G Nachtwei[1], N G Kalugin[1], B E Sağol[1], C Stellmach[1], A Hirsch[1] and G Hein[2]

[1] Institut für Technische Physik, Technische Universität Braunschweig, 38106 Braunschweig, Germany

[2] Physikalisch-Technische Bundesanstalt Braunschweig, 38116 Braunschweig, Germany

Received 28 July 2003
Published 27 February 2004
Online at stacks.iop.org/SST/19/S40 (DOI: 10.1088/0268-1242/19/4/015)

Abstract

Quantum Hall systems can show a bistability in the hysteresis of the breakdown. We realized a relaxation oscillator based on a quantum-Hall device with Corbino geometry. Investigations of the performance of such an oscillator revealed an increase of the hysteresis of the current–voltage curve of the device in comparison with the width of hysteresis at dc voltages. By direct measurements of the hysteresis of the current–voltage curve at different frequencies, we found a marked increase of the breakdown hysteresis at low frequencies of some Hz. We explain the observed dynamical enhancement of the breakdown hysteresis applying an electron heating model with a background (delocalization-related) component of conductivity, which decreases with increasing frequency, indicating a more effective localization already at low frequencies.

In quantum Hall systems, a bistable hysteresis can occur in the current–voltage (I–V) characteristics near the breakdown of the quantum Hall effect (QHE) [1]. This bistability can be applied to generate relaxation oscillations, similar to the negative differential resistance of resonant tunnelling diodes [2]. We developed a simple oscillator circuit with a GaAs/GaAlAs Corbino device. Near the breakdown of the QHE, the Corbino device acts as a bistable switch, which controls the charging and discharging of the circuitry's capacitance (see figure 1). By applying Kirchhoff's equations to the oscillator circuitry, we determined the operational range of parameters of the oscillator [3].

We observed oscillation amplitudes *up to ten times higher* than the breakdown hysteresis as determined from the dc I–V characteristics. To explain this observation, we apply an electron heating model for the QH breakdown [1, 4, 5]. This model attributes the observed strong increase of the dynamical hysteresis to a marked reduction of the background contribution to the conductivity at low frequencies (some Hertz). The reduced background conductivity is related to a reduction of the localization length (and to a more effective localization) in the QH system at low frequencies.

We have patterned circular Corbino devices on a GaAs/GaAlAs heterostructure wafer with an electron density of $n_s = 2.9 \times 10^{11}$ cm^{-2} and a Hall mobility of $\mu_H = 1 \times 10^5$ cm^2 (V s)$^{-1}$. Two types of samples (radius of inner contact—100 μm, radii of outer contact—300 μm (sample A) and 200 μm (sample B)) were investigated. The circuitry of the relaxation oscillator based on the bistable switching of a QH device with Corbino geometry is shown in figure 1. A Corbino device is almost ideally insulating in the QH regime up to a critical value V_{max} of the source–drain voltage V_{SD}. At V_{max}, a sudden onset of the source–drain current I_{SD} occurs. A subsequent reduction of V_{SD} leads to a sudden interrupt of I_{SD} at another critical voltage V_{min} ($V_{min} < V_{max}$). In the hysteresis region $V_{min} < V_{SD} < V_{max}$, the QH device behaves bistably. If a resistance is connected in series and a capacitor as accumulating device in parallel to the QH device (see figure 1), the bistable switching leads to subsequent charging and discharging of the capacitor, detectable as relaxation oscillations.

The amplitude of the relaxation oscillations reflects the width of the *dynamical* hysteresis of the I–V characteristics of the breakdown of the QHE, which we found up to ten times higher than the corresponding *quasi-stationary* one. Therefore, we measured directly the I–V characteristics at low frequencies (up to some hundred Hz) with a two-channel digital oscilloscope.

To characterize the samples, we have measured the Shubnikov–de Haas (SdH) oscillations to determine the carrier

 © 2004 IOP Publishing Ltd Printed in the UK

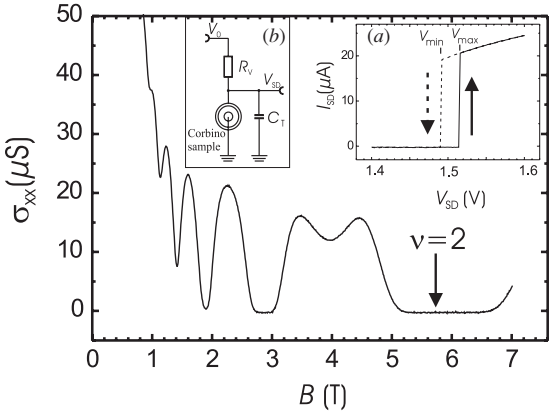

Figure 1. Shubnikov–de Haas oscillations (at $V_{SD} = 100$ mV) of the QH–Corbino devices. Inset: (*a*) dc current–voltage characteristics of the Corbino sample with a channel width of 200 μm at $B = 5.7$ T (second QH plateau, $T = 1.5$ K). (*b*) Scheme of the oscillator circuit: V_0: driving voltage, R_V: serial resistor, C_T: total capacitance.

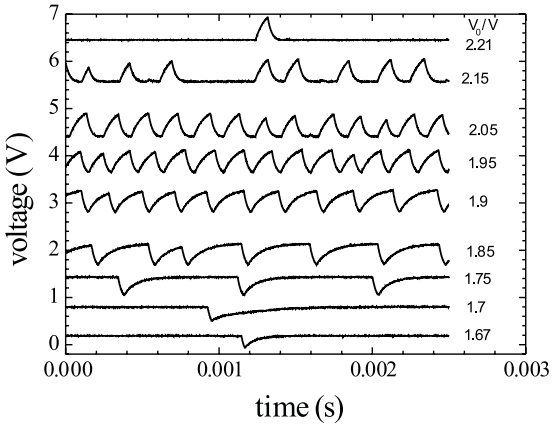

Figure 2. Relaxation oscillations of the Corbino device at different driving voltages V_0 (curves shifted for clarity). $R_{CB} = 90$ kΩ, $R_V = 46$ kΩ, $C_T = 1.5$ nF.

density n_s and the mobility μ_H. The breakdown properties (critical voltages and hysteresis under dc conditions) were determined by measuring the I–V curves at low sweep rates (quasi-stationary conditions). A typical SdH trace and a corresponding breakdown I–V curve (at filling factor 2) are shown in figure 1 and the inset.

After the basic characterization of the samples, we have investigated the oscillator properties of our QH–Corbino devices. The bistable breakdown behaviour of the Corbino device is used for a switch, which closes at V_{max} and opens at V_{min}. The total capacitance (C_T) is charged via the serial resistor R_V until V_{max} (upsweep) is reached. During this process, the Corbino device is insulating and acts like an open switch. The voltage V_{max} closes the switch, and C_T starts to discharge via the Corbino device, which has now a finite resistance R_{CB}. This process endures until the voltage falls to V_{min}, at which point the Corbino device becomes insulating again. Thus, the oscillation amplitude ΔV is determined by the hysteresis, $\Delta V = V_{max} - V_{min}$. Figure 2 shows a set of measured oscillation curves $V_{SD}(t)$ for various values of the driving voltage V_0. The oscillation period T depends on the RC-times τ_{exc} and τ_{rel}, and also on the voltages V_{max}, V_{min} and

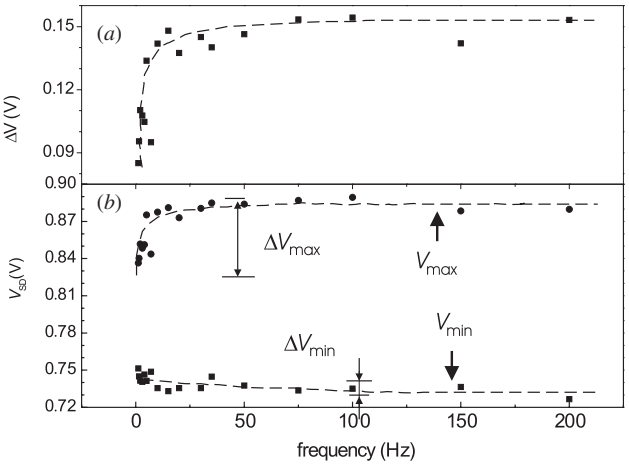

Figure 3. (*a*) The frequency dependence of the amplitude of the QH breakdown hysteresis, (*b*) the frequency dependence of the limits of the hysteresis curve, V_{min} and V_{max} of the Corbino sample with a channel width of 100 μm.

the driving voltage V_0:

$$T = \tau_{exc} \ln\left(\frac{V_0 - V_{min}}{V_0 - V_{max}}\right) + \tau_{rel} \ln\left(\frac{V_{max} - \Theta V_0}{V_{min} - \Theta V_0}\right) \qquad (1)$$

with

$$\Theta = \frac{R_{CB}}{R_{CB} + R_V} \qquad \tau_{rel} = \frac{R_{CB} R_V}{R_{CB} + R_V} \cdot C_T \qquad \tau_{exc} = R_V C_T.$$

The observed amplitudes of the relaxation oscillations (typically $V_{max} - V_{min} = 0.2$–0.4 V, see figure 2) are markedly higher than the dc hysteresis ΔV as deduced from I–V curves under quasi-stationary conditions (see the inset of figure 1).

This increase of the QH breakdown hysteresis inspired us to direct measurements of the hysteresis $\Delta V = V_{max} - V_{min}$ in a wider range of low frequencies. A voltage of sinusoidal waveform, applied to the sample, and the current carried through the Corbino device were monitored by an oscilloscope. The results of the measurements are presented in figure 3. As we see in figure 3(*a*), at low frequencies we observed a growth of the hysteresis amplitude in the region between 0 and 20 Hz, and a saturation at higher frequencies. The experiment shows, that this growth of hysteresis is mainly the result of the growth of V_{max} with increasing frequency, whereas the changes of V_{min} are much less pronounced (figure 3(*b*)).

A common explanation for the observed hysteresis of the current–voltage characteristics of QH devices at the breakdown of the QHE can be derived from the electron heating model [1, 4, 5]. The hysteresis arises from the metastability of the power balance between gain (electrical energy fed to the system), $p_{gain} = \sigma_{xx} E_r^2$ (σ_{xx}—longitudinal conductivity, E_r—radial electric field) and the energy loss rate $p_{loss} = [\varepsilon(T_{el})\text{-}\varepsilon(T_L)]/\tau_{rel}$, which describes the relaxation of the system energy ε at the enhanced electron temperature T_{el} back to the energy at the lattice temperature T_L within the scattering time τ_{rel}. The important point of the model is taking into account the different components of conductivity σ_{xx}:

$$\sigma_{xx}(T_{el}) = \sigma_0 \exp\{-\Delta/(k_B T_{el})\} + \sigma_{BG} \qquad (2)$$

where the first term describes the thermal activation over the Landau gap Δ, and the second term σ_{BG} is the background

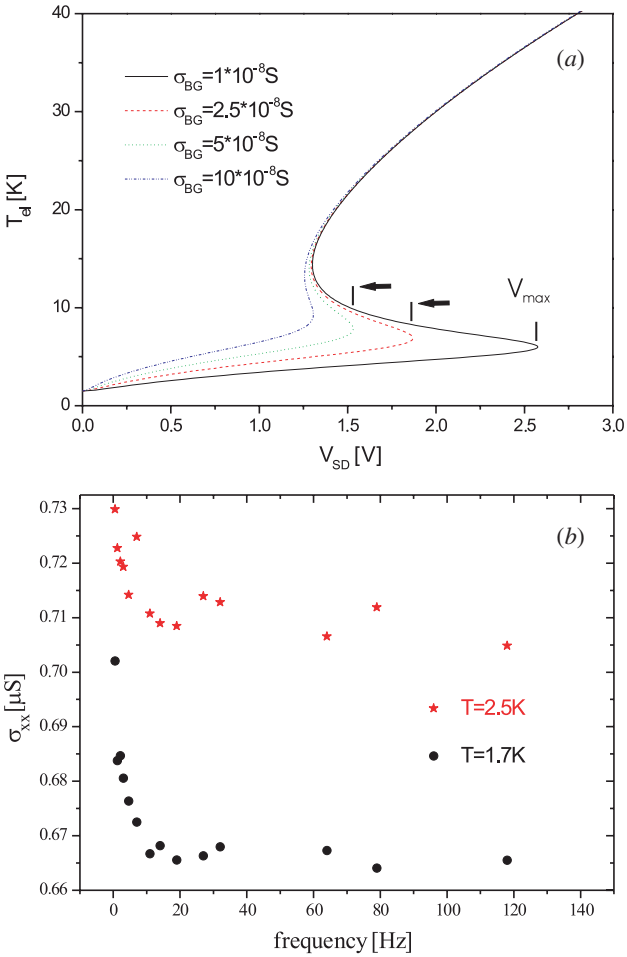

Figure 4. (*a*) Calculated electron temperature T_{el} versus V_{SD} for different background conductivities σ_{BG} for a sample channel width of 200 μm. (*b*) Frequency dependence of the background conductivity in the pre-breakdown regime at a constant voltage (0.8 V) for two temperatures (1.7 K and 2.5 K).

conductivity. The model allows us to describe the appearance and changes of hysteresis in the dependence of T_{el} versus the source–drain voltage V_{SD} (figure 4(*a*)), and, therefore, in the I–V characteristics. The hysteresis values, V_{max} and V_{min}, depend on many parameters, but most essentially on the temperature dependence of $\sigma_{xx}(T_{el})$. The background conductivity, σ_{BG}, is of crucial influence on the breakdown voltage V_{max}. If purely activated behaviour of $\sigma_{xx}(T)$ is assumed, the values for V_{max} become unrealistically high. To obtain values closer to the experiment, additional transport mechanisms leading to finite values of σ_{BG} have to be assumed. Due to the dominance of activated transport at higher electron temperatures, the value of V_{min} is nearly unaffected by the choice of σ_{BG}. The strong drop of σ_{BG} at low frequencies means a pronounced reduction of the localization length. In other words, the localization of electrons near local potential fluctuations becomes more effective already at low frequencies, as compared to the case of constant electric fields.

To verify these model assumptions, we investigated the frequency dependence of the conductivity in the pre-breakdown regime. The data in figure 4(*b*) were taken for a constant voltage of 0.8 V (smaller than the dc-breakdown voltage V_{max} of 1.5 V here) at two different temperatures, and a steep decrease of the conductivity with increasing frequency, which supports qualitatively the assumptions made in the electron heating model, is visible. It is obvious that the behaviour of the curves is qualitatively similar to figure 3 (a reduction of the background conductivity leads to an increase of V_{max}).

To summarize, we have generated relaxation oscillations applying a quantum Hall Corbino device as a bistable switching element. The oscillation amplitude is determined by the dynamical hysteresis of the QH device. The frequency of the oscillation depends on the resistances and capacitances of the circuit, but also on the dynamical hysteresis of the Corbino device. This hysteresis is determined by the dynamical breakdown properties of the device and can be directly deduced from the measurements. Direct measurements of the hysteresis confirmed a steep increase of the dynamical hysteresis at low frequencies. A hot electron model used to explain this finding leads to the assumption of a corresponding strong decrease of the background conductivity, which was experimentally confirmed in the pre-breakdown regime.

Acknowledgments

This work was supported by the Schwerpunktprogramm ‘Quanten-Hall-Systeme’ of the Deutsche Forschungsgemeinschaft (DFG), Project NA235/10–2. AB thanks F Hohls, F Schulze Wischeler and R Haug for the support of his measurements. BES acknowledges the support of the Deutscher Akademischer Austauschdienst (DAAD).

References

[1] Ebert G *et al* 1983 *J. Phys. C: Solid State Phys.* **16** 5441
[2] Brown E R *et al* 1991 *Appl. Phys. Lett.* **58** 2291
[3] Nachtwei G *et al* 2003 *Appl. Phys. Lett.* **82** 2068
[4] Komiyama S *et al* 1985 *Solid State Commun.* **54** 479
[5] Nachtwei G *et al* 1998 *Phys. Rev.* B **57** 9937